



Simultaneous Frequency and Amplitude Estimation for Grid Quality Monitoring : New Partitioning with Memory Based Newton-Schulz

Downloaded from: <https://research.chalmers.se>, 2025-12-09 23:30 UTC

Citation for the original published paper (version of record):

Stotsky, A. (2022). Simultaneous Frequency and Amplitude Estimation for Grid Quality Monitoring : New Partitioning with Memory Based Newton-Schulz Corrections. IFAC-PapersOnLine, 55(9): 42-47.
<http://dx.doi.org/10.1016/j.ifacol.2022.07.008>

N.B. When citing this work, cite the original published paper.

Simultaneous Frequency and Amplitude Estimation for Grid Quality Monitoring : New Partitioning with Memory Based Newton-Schulz Corrections ^{*}

Alexander Stotsky ^{*}

^{}Department of Computer Science and Engineering, Chalmers University and
University of Gothenburg, SE-412 96 Gothenburg, Sweden
e-mail: alexander.stotsky@chalmers.se*

Abstract: High penetration level of renewable energy sources and introduction of controllable loads will result in significant harmonic emissions and sag and swell events in the future electricity networks. Development of the methods for high performance simultaneous estimation of the frequency and amplitude events is required for stable operation of the future electricity networks since zero crossing frequency detection method (which is widely used nowadays in industry) is not accurate enough and does not allow estimation of the amplitude events. The multiple model method which is suitable for simultaneous estimation of the frequency and amplitude is extended in this paper with introduction of a new decomposition technique based on stepwise partitioning, which allows simultaneous construction and accurate and computationally efficient inversion of the information matrix. Recursive calculations of the inverse introduce error accumulation and a new general high order memory based Newton-Schulz iteration is proposed in this paper for correction and reduction of the accumulated error. Moreover, parallel Richardson iterations which are based on partitioning method are proposed in this paper for reduction of the computational complexity. The methods are especially efficient for approximation of the signals with large number of harmonics. The approaches were tested for simultaneous estimation of the frequency and sag and swell signatures in the one-phase synchronized voltage waveform measured at the wall outlet. Simulation results show that the multiple model method provides more accurate frequency estimation in comparison to zero crossing method.

In addition, the cascade multiple model method which is based on the multi-windowing technique (where the components of the signals are separated via a proper choice of the window sizes) is introduced in this paper for estimation of the significantly separated frequencies of the electrical signals. The approach was tested in the problem of frequency estimation using the measurement record from the electric vehicle with on-board charger connected to the supply voltage in the laboratory.

Copyright © 2022 The Authors. This is an open access article under the CC BY-NC-ND license (<https://creativecommons.org/licenses/by-nc-nd/4.0/>)

Keywords: Simultaneous Estimation of the Frequency and Amplitudes for Power Quality Monitoring, Recursive Partitioning, General Memory Based High Order Newton-Schulz Algorithms, Parallel Richardson Iterations, Cascade Multiple Model, Multi-Windowing Technique

1. INTRODUCTION

Additional significant distortions of voltage and current signals are expected in the future electricity networks due to higher penetration level of renewable energy sources, modern power electronics, non-linear controllable loads and many others. These distortions result in significant deviations from the fundamental network frequency, appearance of a large number of harmonics and significant sag and swell events in the network signals. Zero crossing frequency detection method (Friedman, 1994) and its modifications is not accurate enough for frequency estimation in the presence of large number of harmonics and does not allow estimation of the sag and swell events.

This necessitates the development of the computationally efficient methods for simultaneous estimation of the frequency and amplitude events in the future electricity networks. One of the promising approaches to simultaneous frequency and amplitude estimation is the multiple model method described in Stotsky (2016), where the survey of existing frequency estima-

tion methods was also presented. The frequency in this method is estimated using spline based estimation of the variance, whereas the amplitudes are estimated with the least squares method. Application of the multiple model (which consists of a relatively large number of models) requires significant computational efforts, especially for a large number of harmonics. The most significant computational burden is associated with calculation and inversion of the large scale information matrix with large condition number. In other words the development of new numerical decomposition methods for matrix inversion and parameter estimation for large scale systems is required, Stotsky (2015, 2019).

A new decomposition method based on stepwise partitioning, which allows simultaneous construction and computationally efficient and accurate inversion of the information matrix is proposed in this paper. Recursive calculations of the inverse introduce error accumulation and a new general high order memory based Newton-Schulz iteration is introduced in this paper (as generalization of the memory based algorithm described in Stotsky, 2022) for error reduction.

^{*} This work was not supported by any organization

Computational resources with high degree of parallelism will be available in the future and new parallel Richardson iterations which are based on the partitioning method are proposed in this paper for reduction of the computational complexity. The approaches were tested for simultaneous estimation of the frequency and sag and swell signatures in the one-phase synchronized voltage waveform measured at the wall outlet.

The second part of the paper is devoted to the extension of the multiple model method. Many multi-frequency signals in electrical systems have significant separation between the frequencies. Such signals can not be accurately approximated using conventional approaches due to the large differences in the frequencies. In other words, one window size which accurately estimates both low and high frequency components does not exist. Therefore the cascade approach which allows application of different window sizes should be developed for accurate signal approximation.

Known methods, such as EMD (Empirical Mode Decomposition) method, Altintas et al. (2019), applied often for evaluation of the modulation effect are based on construction of the envelope associated with maximal and minimal values of the signal. The method has significant computational complexity associated with calculation of the extreme values and does not provide sufficient accuracy of estimation in the presence of the measurement noise due to inaccurate determination of the envelope.

A new robust cascade estimation method based on the multiple model concept is developed in this paper. The method allows accurate estimation of the frequencies and amplitudes by applying multi-windowing technique, where the components of the signals are separated via a proper choice of the window sizes. The approach was tested for estimation of two significantly separated frequencies in the measurement record of the electric vehicle with on-board charger connected to the supply voltage in the laboratory.

2. ESTIMATION WITH MULTIPLE MODEL

Suppose that the measured signal y_k is presented in the following form :

$$y_k = \varphi_k^T \theta_* + \xi_k \quad (1)$$

where θ_* is the vector of unknown parameters and φ_k is unknown harmonic regressor:

$$\varphi_k^T = [\cos(q_0 k) \sin(q_0 k) \cos(2q_0 k) \sin(2q_0 k) \dots \cos(hq_0 k) \sin(hq_0 k)] \quad (2)$$

where q_0 is unknown fundamental frequency of the network (for example, $q_0 = 50$ Hertz or $q_0 = 60$ Hertz), h is unknown number of harmonics, and ξ_k is a zero mean white Gaussian noise, $k = 1, 2, \dots$ is the step number. The system has four unknown quantities : 1) the fundamental frequency of network q_0 , 2) the number of harmonics h , which can be large in the future electricity networks, 3) the vector of the parameters θ_* , and 4) the variance of the measurement noise, ξ_k . It is assumed that the upper bound \bar{h} of the number of harmonics is known, $h \leq \bar{h}$.

The algorithm for simultaneous frequency and parameter estimation (the algorithm estimates all four unknown quantities mentioned above) is described in Stotsky (2016), where the estimates of the regressor vector $\hat{\varphi}_i$ are introduced for a number of fundamental frequencies i (with corresponding number of harmonics, \bar{h}), which cover actual frequency. The variance of the measurement noise is calculated for each regressor and the

estimated frequency corresponds to the minimal value of the estimated variance. For estimation of the variance the following large scale system (for a large number of harmonics) $A_i \theta_i = b_i$, where $A_i = \sum_{j=k-(w-1)}^{j=k} \hat{\varphi}_{ij} \hat{\varphi}_{ij}^T$ is SPD (Symmetric Positive Definite) information matrix for regressor $\hat{\varphi}_i$ and w is the window size, $k \geq w$, should be solved with sufficiently high accuracy in each step with respect to θ_i . Notice that accurate estimation of rapidly changing frequencies and amplitudes is possible with sufficiently small window size only, which results in ill-conditioned matrices A_i .

The accuracy requirements is the main motivation for application of the Richardson algorithms for estimation of the parameter vector θ_i . Since the convergence of the Richardson iteration can be slow especially for ill-conditioned and large scale case the development of computationally efficient procedure for construction and inversion of the information matrix is required. Stepwise algorithm which is based on partitioning and deals with submatrices with significantly smaller condition numbers (the condition numbers are reduced by several thousand times) is presented in the next Section 3. The algorithm allows simultaneous construction and inversion of the information matrix.

3. RECURSIVE PARTITIONING AND CALCULATION OF THE INVERSE

3.1 Description of the Method

Consider the following partitioning:

$$A = \sum_{j=k-(w-1)}^{j=k} \hat{\varphi}_j \hat{\varphi}_j^T = \begin{bmatrix} \begin{bmatrix} P_1 & B_1 \\ B_1^T & C_1 \end{bmatrix} & \dots & B_z \\ \vdots & \ddots & \vdots \\ B_z^T & & C_z \end{bmatrix}$$

where SPD information matrix A^1 is calculated in a moving window of a size w , where the regressor vector φ contains trigonometric functions. Calculation of the matrix inverse is based on the sequential inversion of positive definite upper left submatrices :

$$\begin{bmatrix} P_r & B_r \\ B_r^T & C_r \end{bmatrix}^{-1} = \begin{bmatrix} I & \hat{X}_r \\ 0 & I \end{bmatrix} \begin{bmatrix} \hat{P}_r^{-1} & 0 \\ 0 & \hat{S}_r^{-1} \end{bmatrix} \begin{bmatrix} I & 0 \\ \hat{X}_r^T & I \end{bmatrix} \quad (3)$$

where $\hat{X}_r = -\hat{P}_r^{-1} B_r$, $\hat{S}_r = C_r - B_r^T \hat{P}_r^{-1} B_r$, and \hat{P}_r^{-1} is an estimate of the inverse of the matrix $P_r = P_r^T > 0$ is known from the previous step, where $r = 1, 2, \dots$ is the step number. The inversion formula (3) can be found in Stotsky (2015).

In other words, the recursive inversion procedure starts with the

partitioning of the matrix $\begin{bmatrix} P_1 & B_1 \\ B_1^T & C_1 \end{bmatrix}$ which corresponds to the initial set of the harmonics and calculation of the inverse of P_1 . Notice that the positive definite matrix P_1 has low condition number and can be easily inverted. The initial number of harmonics should not be chosen large, which results in a small

¹ Any SPD matrix can be partitioned as $A = \begin{bmatrix} P & B \\ B^T & C \end{bmatrix}$ where P and C are square. The matrix can be transformed to the block-diagonal form using the following transformation matrix $T = \begin{bmatrix} I & 0 \\ X^T & I \end{bmatrix}$ where $X = -P^{-1}B$ and I is the identity matrix. The block diagonal decomposition can be presented as $T A T^T = \begin{bmatrix} P & 0 \\ 0 & S \end{bmatrix}$, where $S = C - B^T P^{-1} B > 0$, $P > 0$, Horn & Johnson (1985), Theorem 7.7.6

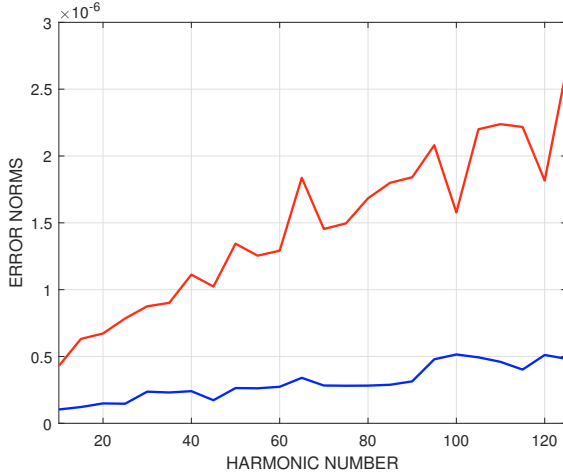


Figure 1. The error norm $\|I - \hat{H}^{-1}H\|_{\infty}$, where $H = \begin{bmatrix} P_r & B_r \\ B_r^T & C_r \end{bmatrix}$ and \hat{H}^{-1} is calculated using (3), is plotted with a red line in every step of the inversion of the information matrix. After application of the correction algorithm described in Section 3.2 the same norm is plotted with the blue line, which shows significant improvement of the inversion accuracy.

size of the matrix P_1 . The inverse of the partitioned matrix is easily calculated using (3), where the matrix \hat{S} of the reduced size is inverted only. Then the partitioned matrix becomes positive definite upper left submatrix, whose inverse is known for the second step. The final step of the procedure corresponds to accommodation of all \bar{h} harmonics, and simultaneous calculation of the information matrix and its inverse, whereas the matrix \hat{S} of the reduced size and condition number is inverted only in each step. Indeed, stepwise matrix order reduction results in reduction of the condition numbers of the matrices (the condition number of the matrix \hat{S}_r in every step is approximately ten thousand times less than the condition number of the matrix A), which in turn results in significant improvement of the inversion accuracy in each step and improvement of the accuracy of the inverse of the information matrix at the final step. The estimate \hat{A}^{-1} of the inverse of matrix A is used for parameter calculation in the following Richardson iteration $\vartheta_k = \vartheta_{k-1} - \hat{A}^{-1} \{A\vartheta_{k-1} - b\}$, where ϑ_k is estimate of the parameter vector θ which satisfy large scale algebraic equation $A\theta = b$ and the spectral radius $\rho(I - \hat{A}^{-1}A) \ll 1$, Stotsky (2019). Application of the Richardson iteration is absolutely necessary for improvement of the accuracy of the estimated parameters which has the direct impact on the accuracy of the estimated variance and frequency. Another application of the partitioning method which results in computationally efficient parallel Richardson iterations is described in Section 4.

3.2 Error Accumulation and Reduction

The method described above has been tested for stepwise construction and inversion of the information matrix with 125 harmonics where five harmonics were added in each step with monitoring of the inversion error. Inversion error is plotted in Figure 1 with a red line, which shows error accumulation as a function of the harmonic number, which can be seen as main drawback of this method. Notice that the inversion accuracy can be improved via iterative corrections using Newton-Schulz algorithms applied in each step for calculation of the inverses

of the matrices \hat{S}_r^{-1} in (3) and $\begin{bmatrix} P_r & B_r \\ B_r^T & C_r \end{bmatrix}^{-1}$ with preconditioner defined in (3). High order Newton-Schulz iteration is a powerful tool for calculation and correction of the inverses of the matrices. One step of correction with Newton-Schulz iteration (which has minimal computational complexity) is sufficient for significant improvement of the inversion accuracy.

A new general high order Newton-Schulz iterative method is proposed in this Section for the accuracy improvement. A new memory based convergence accelerator is integrated in the high order Newton-Schulz iterative method, where the estimate in the step k is calculated using the estimates from the steps $k-1$ and $k-2$ and the error model (constructed via a proper choice of the algorithm parameters) accumulates multiplicatively inversion errors calculated in the previous steps aiming for convergence rate improvement. The method can be written in the following form:

$$F_{k-1}^n = I - \sum_{j=0}^{n-1} F_{k-1}^j G_{k-1} A \quad (4)$$

$$G_k = G_{k-1} + \underbrace{P_{k-1} \left\{ \sum_{j=0}^m F_{k-1}^j \sum_{j=0}^{n-1} F_{k-1}^j G_{k-1} - \sum_{j=0}^{nm+n-1-q} F_{k-2}^j G_{k-2} \right\}}_{\sum_{j=0}^{nm+n-1} F_{k-1}^j G_{k-1}} \quad (5)$$

$$P_k = P_{k-1} F_{k-1}^q, \quad P_1 = F_0^q \quad (6)$$

$$F_k = I - G_k A = P_{k-1} F_{k-1}^{nm+n} = \underbrace{F_0^q F_1^q \cdots F_{k-2}^q}_{\text{Memory Based Convergence Accelerator}} F_{k-1}^{nm+n} \quad (7)$$

where $G_1 = \sum_{j=0}^m F_0^j \sum_{j=0}^{n-1} F_0^j G_0$ and the preconditioner G_0 is taken

from the partitioning method (3), $n = 1, 2, \dots, m = 0, 1, \dots$ and $q = 0, \dots, nm + n - 1$ are the parameters of the algorithm which specify the error model (7), $k = 2, 3, \dots$. This error model is obtained by multiplication of (5) by A which results in the following error model $F_k = F_{k-1} + P_{k-1} \{F_{k-1}^{nm+n} - F_{k-2}^{nm+n-q}\}$ with subsequent evaluation of P_{k-1} using (6).

Different combinations of the parameters n, m and q result in different algorithms. For example, the case with $m = 1$ and $q = n$ is described in Stotsky (2022) and the case with $q = 0$ where $P_k = I$ results in classical high order Newton-Schulz algorithm, Isaacson & Keller (1966). Notice also that the choice of q has the direct impact on the memory based convergence accelerator and in turn on the error model and the convergence rate. For example, the algorithm with the parameter combination $n = 1, m = 0$ and $q = 0$ does not converge.

Notice that the factorization methods can be applied directly to the power series $\sum_{j=0}^{nm+n-1} F_{k-1}^j G_{k-1}$ and the algorithm can be divided into independent computational parts for efficient parallel implementation.

The matrix G_2 , ($k = 2$), calculated via (5) with the parameters $n = 2, m = 1$ and $q = n$ is used as corrected estimate of the matrix inverses in Section 3.1. This correction method has been tested for reduction of the inversion errors which are plotted in Figure 1. The inversion errors before and after correction are plotted with the red and blue lines respectively.

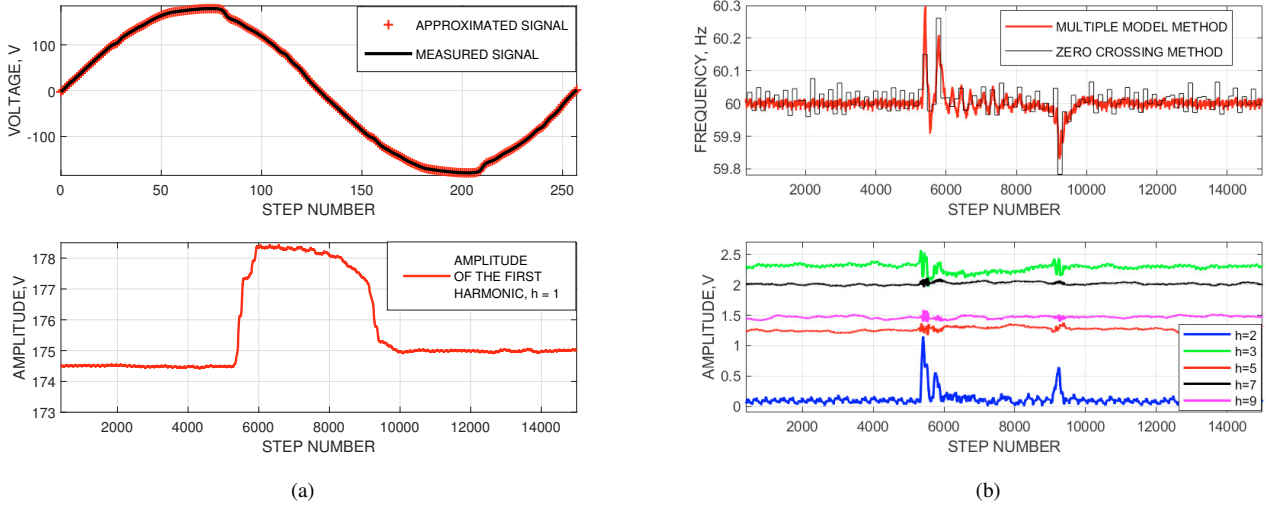


Figure 2. Measured voltage signal and its multiple model approximation (with five models and 120 harmonics) are plotted in the first plot of the Figure (a) with the black line and plus signs respectively. Two frequency estimation methods are compared in the first plot of the Figure (b), where the curves for multiple model and zero crossing method are plotted with red and black lines respectively. The amplitude of the first harmonic is plotted in the second plot of the Figure (a). The amplitudes of the first most essential harmonics are plotted in the second plot of the Figure (b).

4. PARTITIONING BASED PARALLEL RICHARDSON ITERATIONS

Another application of the partitioning method for estimation of the parameter vector θ which satisfy large scale algebraic equation $A\theta = b$ is considered in this Section. The SPD information matrix A is partitioned as follows $A = \begin{bmatrix} P & B \\ B^T & C \end{bmatrix}$, where P and C are square of approximately the same size. Introduction of a new parameter vector δ such that $\theta = T^T \delta$, where $T = \begin{bmatrix} I & 0 \\ X^T & I \end{bmatrix}$ and $X = -P^{-1}B$ results in the transformation of the algebraic equation to the block diagonal form $TAT^T \delta = Tb$, where $TAT^T = \begin{bmatrix} P & 0 \\ 0 & S \end{bmatrix}$, and $S = C - B^T P^{-1}B$ which in turn allows partitioning of the vector $\delta = [\delta_1 \ \delta_2]^T$ and $\beta = Tb = [\beta_1 \ \beta_2]^T$. The components δ_1 and δ_2 of the parameter vector δ can be independently estimated in two parallel Richardson loops:

$$\begin{aligned} \vartheta_{1k} &= \vartheta_{1k-1} - \hat{P}^{-1} \{P \vartheta_{1k-1} - \hat{\beta}_1\}, \quad \vartheta_{10} = \hat{P}^{-1} \hat{\beta}_1 \\ \vartheta_{2k} &= \vartheta_{2k-1} - \hat{S}_k^{-1} \{\hat{S} \vartheta_{2k-1} - \hat{\beta}_2\}, \quad \vartheta_{20} = \hat{S}_0^{-1} \hat{\beta}_2 \end{aligned}$$

where $\hat{\beta} = \hat{T}b$, $\hat{T} = \begin{bmatrix} I & 0 \\ \hat{X}^T & I \end{bmatrix}$ and $\hat{X} = -\hat{P}^{-1}B$, $\hat{\beta}_1 = \beta_1$, $k =$

$1, 2, \dots$. The approximate inverse \hat{S}_k^{-1} of the matrix $\hat{S} = C - B^T \hat{P}^{-1}B$ is calculated recursively inside of the Richardson algorithm using high order Newton-Schulz method described in Section 3.2, Stotsky (2022). The estimate \hat{P}^{-1} of the inverse of the matrix P is calculated beforehand using the same method. Finally, the estimate of the parameter vector is calculated as follows $\hat{\theta} = \hat{T}^T \vartheta$, where $\vartheta = [\vartheta_1 \ \vartheta_2]^T$.

This algorithm provides significant computational savings due to parallel implementation and it is especially efficient for systems with ill-conditioned matrix A of the large size since the matrix P of the reduced size and condition number is inverted only and the approximate inverse \hat{S}_k^{-1} is applied for the improvement of the convergence rate of the Richardson iteration.

5. SIMULTANEOUS ESTIMATION OF THE FREQUENCY AND AMPLITUDE EVENTS ON REAL DATA

Multiple model approach described above was tested for simultaneous estimation of the frequency and sag and swell signatures on real data from the electricity network. The one-phase synchronized voltage waveform measured at the wall outlet (approximately 120V RMS) is used for verification. The sampling measurement rate is 256 points per cycle. Simulation results are presented in Figure 2, which shows simultaneous occurrence of the frequency and sag/swell events.

The first plot in the Figure 2(a) shows approximation performance of the multiple model approach for five models and 120 harmonics, where measured voltage signal and multiple model approximation are plotted with the black line and plus signs respectively. The Figure 2(a) shows that the signal is well approximated with 120 harmonics in one cycle.

Two frequency estimation methods are compared in the first plot of the Figure 2(b), where the curves for multiple model and zero crossing method are plotted with red and black lines respectively. The curves show that the multiple model method provides more accurate frequency estimation in comparison to zero crossing method. Moreover, multiple model method is suitable for detection of the sag and swell events, which is not possible with zero crossing method. Indeed, the second plot of the Figure 2(a) shows the voltage swell (which is a momentary increase in voltage that occurs usually when a heavy load turns off in the system) on the amplitude of the first harmonic. Finally, the amplitudes of the first most essential harmonics are plotted in the second plot of the Figure 2(b), which confirms simultaneous occurrence of the frequency and amplitude events.

In addition, the simulation results show that zero crossing algorithm accumulates errors for sufficiently large measurement records. Error accumulation problem can be solved by introduction of the local coordinates, Stotsky (2016). Parameter calculation method based on LU decomposition does not provide accurate results in the multiple model method for ill-conditioned information matrices. The accuracy of the parameter calculation was improved by application of the Richardson method.

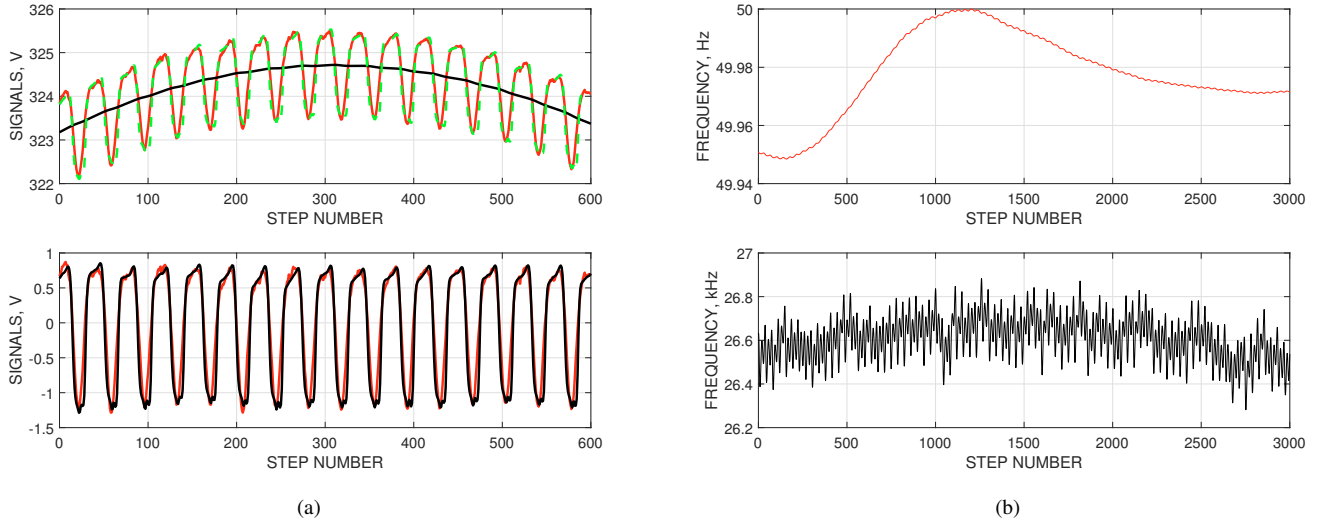


Figure 3. The first plot of the Figure (a) shows measured signal plotted with the red line and its approximation plotted with the green dash line. Estimated low frequency component of the signal is plotted with a black line. The error between the signal and its low frequency component is plotted with a red line on the second plot of the Figure (a) and its approximation is plotted with a black line. The frequency estimates are plotted in the first and second plots respectively of the Figure (b).

6. MULTIPLE MODEL IN CASCADE FREQUENCY ESTIMATION

Suppose that multi-frequency signal y_k can be presented in the following composite form :

$$y_k = p_0 + p_1 + \dots + p_m + \xi_k = \sum_{i=0}^m p_i + \xi_k \quad (8)$$

$$p_i = \phi_i^T \theta_{*i} \quad (9)$$

$$\phi_i^T = [1 \cos(q_i k) \sin(q_i k) \dots \cos(n_i q_i k) \sin(n_i q_i k)] \quad (10)$$

where p_i represent the parts of the signal associated with the frequencies q_i and higher harmonics n_i , $\theta_{*i} = \theta_{*ik}$ is the vector of unknown time varying parameters, $i = 0, 1, \dots, m$, ξ_k is a zero mean white Gaussian noise and $k = 1, 2, \dots$ is the step number. The signal has $m + 1$ fundamental (main) time varying frequencies, where each frequency has its own higher harmonics. The time varying frequencies $q_i = q_{ik}$ are well separated from each other, and q_{0k} is the lowest frequency. Notice that the regressor vector (10) may contain overtones of the frequencies q_i instead of higher harmonics. The frequencies q_i , higher harmonics n_i , parameters θ_{*i} and the noise ξ_k are unknown. It is assumed that the upper bounds of the numbers of the harmonics \bar{n}_i are known. Notice that the signals presented in the form (8) can not be accurately approximated using conventional approaches due to the large differences in frequencies. In other words, both low and high frequency components of the signal can not be accurately estimated using one window size (in the case of estimation in the moving window). Therefore the cascade approach which allows application of different window sizes should be developed for accurate approximation of the signal and tracking of the frequencies.

The signal (8) can be presented in the following cascade form:

$$y_{i+1} = y_i - p_i, \quad y_0 = y_k, \quad i = 0, 1, \dots, m-1 \quad (11)$$

and the components p_i and y_i of the signal y_0 are estimated separately as follows:

$$\hat{p}_i = \phi_i^T \theta_i, \quad \hat{y}_{i+1} = \hat{y}_i - \hat{p}_i, \quad \hat{y}_0 = y_0, \quad \hat{p}_i \approx p_i \quad (12)$$

$$\phi_i^T = [1 \cos(\hat{q}_i k) \sin(\hat{q}_i k) \dots \cos(\bar{n}_i \hat{q}_i k) \sin(\bar{n}_i \hat{q}_i k)] \quad (13)$$

$$A_i \theta_i = b_i \quad (14)$$

$$A_i = \sum_{j=k-(w_i-1)}^{j=k} \phi_{ij} \phi_{ij}^T, \quad k \geq w_i \quad (15)$$

$$b_i = \sum_{j=k-(w_i-1)}^{j=k} \phi_{ij} \hat{y}_i \quad (16)$$

$$\hat{y}_k = \hat{p}_0 + \hat{p}_1 + \dots + \hat{p}_m = \sum_{i=0}^m \hat{p}_i \quad (17)$$

$$v = \frac{\sum_{j=k-(w_m-1)}^{j=k} (\hat{y}_{mj} - \hat{p}_{mj})^2}{w_m - n_{\theta_m} - 1} \quad (18)$$

where the parameter vector θ_i in (12) is estimated using the least squares method as the solution of the algebraic equation (14) with symmetric and positive definite information matrix A_i defined in (15). The frequencies \hat{q}_i are estimated with the multiple model method, see Section 2 and Stotsky (2016). The regressor vector ϕ_i , (13) contains estimated frequencies \hat{q}_i , and the window size w_i is selected according to the frequencies. Such selection captures different components of the signal for accurate approximation. For example, a sufficiently large window size w_0 is selected for the lowest frequency q_0 . Large window size filters out all high frequency components of the signal, q_i , $i = 1, 2, \dots$ and their harmonics. Each subsequent window size should be chosen smaller than the previous one, providing filtering for the corresponding frequencies.

The signal y_k in (8) is approximated component-wise by \hat{y}_k in (17) and the variance of the measurement noise is estimated in the last step of the process via (18), where w_m is the smallest window size and n_{θ_m} is the number of estimated parameters. Notice that the variance of the approximation error can be estimated in each step of the algorithm. The variance is reduced in each step and the number steps can be increased until the

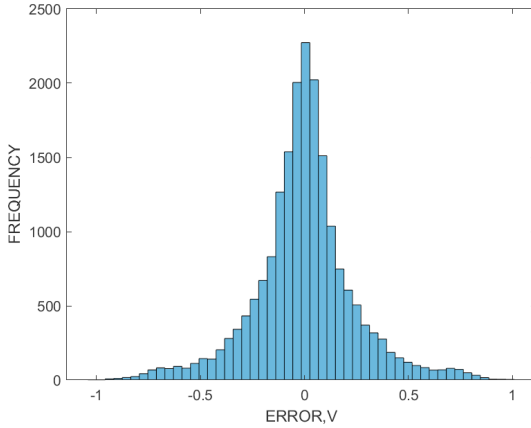


Figure 4. Histogram of the residual error.

reduction of the variance (which can be verified using the test for equal variances) is not statistically significant. The test for equal variances determines stopping criteria for the algorithm.

6.1 Processing of the Measurement Record on Electric Vehicle

The approach presented above is illustrated on the measurement record of EV (Electric Vehicle) with on-board charger connected to the supply voltage in the laboratory. The nominal frequency of the supply source is 50 Hz with the voltage level of 230 V (RMS). The single-phase voltage was recorded over two seconds with the sampling rate of 1 MHz. The data was provided by European Metrology, (2019).

The waveform includes EMI (Electromagnetic Interference) with the switching frequency of a charger (at approximately 27 kHz) and its second harmonic.

The model of the signal is presented in the form (8) with $m = 1$, where the regressor φ_0 contains only two trigonometric functions, without high order harmonics, $n_0 = 1$ and the signal p_1 contains the frequency of a charger (approximately 27 kHz) and its second harmonic. The signal is approximated as follows:

$$\hat{y}_k = \hat{p}_0 + \hat{p}_1 \quad (19)$$

$$\hat{p}_0 = \varphi_0^T \theta_0, \quad y_0 = y_k \quad (20)$$

$$\varphi_0^T = [\cos(\hat{q}_0 k) \sin(\hat{q}_0 k)] \quad (21)$$

$$\hat{p}_1 = \varphi_1^T \theta_1, \quad \hat{y}_1 = y_k - \hat{p}_0 \quad (22)$$

$$\varphi_1^T = [1 \cos(\hat{q}_1 k) \sin(\hat{q}_1 k) \cos(\bar{n}_1 \hat{q}_1 k) \sin(\bar{n}_1 \hat{q}_1 k)] \quad (23)$$

where \hat{y}_k is approximation of the signal y_k defined in (8). The signals \hat{p}_0 and \hat{p}_1 are approximations of the components p_0 and p_1 respectively. The component \hat{p}_0 is estimated via (20) where \hat{q}_0 is estimated using multiple model approach, and the parameter vector θ_0 is calculated using the least squares method with the sufficiently large window size, $w_0 = 8000$. The difference $\hat{y}_1 = y_k - \hat{p}_0$ is the input to the next step where the model \hat{p}_1 is defined in (22). The model contains the frequency \hat{q}_1 estimated using multiple model and the parameter vector θ_1 , which contains the offset parameter for compensation of the approximation errors in the previous step. The parameter vector is estimated using the least squares method with $\bar{n}_1 = 2$ and the window size $w_1 = 50 \ll w_0$.

Simulation results of the system (19) - (23) are presented in Figure 3. The first plot of the Figure 3(a) shows measured signal plotted with the red line and its approximation (which is calculated via the model (19)) plotted with the green dash line.

Estimated low frequency component \hat{p}_0 of the signal is plotted with a black line. The error $\hat{y}_1 = y_k - \hat{p}_0$ is plotted with a red line on the second plot of the Figure 3(a) and its approximation \hat{p}_1 calculated using (22) is plotted with a black line. Finally, the frequency estimates \hat{q}_0 and \hat{q}_1 estimated using the cascade multiple model approach are plotted in the first and second plots respectively of the Figure 3(b). Histogram of the residual error which represents the measurement noise is plotted in Figure 4.

7. CONCLUSIONS

Significant wave form distortions and harmonic emissions which are expected in the future networks necessitate the development of fast, accurate and computationally efficient methods for frequency and amplitude estimation. This paper offers new computationally efficient tool-kit for simultaneous frequency and amplitude estimation within the multiple model concept for large scale systems. The tool-kit includes stepwise partitioning with corrections for construction and inversion of the information matrix and partitioning based parallel Richardson algorithms. Simulation results on the measurement record show that the multiple model method provides more accurate frequency estimation in comparison to zero crossing method and high performance detection of the sag and swell events via accurate estimation of the amplitudes.

In addition, the multiple model concept was extended in this paper and new cascade method based on multi-windowing technique was introduced. Simulation results on the measurement record of the electric vehicle confirmed that the method provides accurate stepwise estimation of the significantly separated frequencies.

REFERENCES

- [1] Altintas A., Davidson L. and Peng S. (2019). A New Approximation to Modulation Effect Analysis Based on Empirical Mode Decomposition, *Phys. Fluids* 31, 025117.
- [2] European Metrology, project 18NRM05, SupraEMI (2019 – 2022), <http://empir.npl.co.uk/supraemi/>
- [3] Friedman V. (1994). A Zero Crossing Algorithm for the Estimation of the Frequency of a Single Sinusoid in White Noise, *IEEE Transactions on Signal Processing*, vol. 42, No. 6, pp. 1565-1569.
- [4] Horn R. and Johnson C. (1985). *Matrix Analysis*, Cambridge University Press.
- [5] Isaacson E. and Keller H. (1966). *Analysis of Numerical Methods*, John Wiley & Sons, New York.
- [6] Stotsky A. (2015). Accuracy Improvement in Least-Squares Estimation with Harmonic Regressor: New Pre-conditioning and Correction Methods, 54-th CDC, Dec. 15-18, Osaka, Japan, pp. 4035-4040.
- [7] Stotsky A. (2016). Towards Accurate Estimation of Fast Varying Frequency in Future Electricity Networks: The Transition from Model-Free Methods to Model-Based Approach, *Journal of Systems and Control Engineering*, vol. 230, N 10, pp. 1164-1175.
- [8] Stotsky A. (2019). Unified Frameworks for High Order Newton-Schulz and Richardson Iterations: A Computationally Efficient Toolkit for Convergence Rate Improvement, *JAMC*, vol. 60, N 1 - 2, pp. 605-623.
- [9] Stotsky A. (2022). Recursive Versus Nonrecursive Richardson Algorithms: Systematic Overview, *Unified Frameworks and Application to Electric Grid Power Quality Monitoring, Automatika*, vol. 63, N2, pp. 328-337, <https://doi.org/10.1080/00051144.2022.2039989>